Ultrafast All-Optical Polarization Switch Controlled by Optically Excited Picosecond Acoustic Perturbation of Exciton Resonance in Planar Microcavities

A.A. Demenev,[1] D.D. Yaremkevich,[2] A.V. Scherbakov,[2,*] S.S. Gavrilov,[1,3] D.R. Yakovlev,[2,4] V.D. Kulakovskii,[1,†] and M. Bayer[2]

[1] *Institute of Solid State Physics, Russian Academy of Sciences, Chernogolovka 142432, Russia*
[2] *Experimentelle Physik 2, Technische Universität Dortmund, Dortmund D-44227, Germany*
[3] *National Research University Higher School of Economics, Moscow 101000, Russia*
[4] *Ioffe Institute, Russian Academy of Sciences, St. Petersburg 194021, Russia*

(Received 5 April 2022; revised 17 July 2022; accepted 22 August 2022; published 19 October 2022)

All-optical switching of the polarization of exciton polaritons is studied using a picosecond acoustic perturbation of the exciton resonance in high-Q planar GaAs/AlAs microcavities. An irreversible switching of the degree of circular polarization from 22% up to 82% is realized in a microcavity pumped by a laser with a photon energy slightly exceeding the lower polariton resonance. The polarization switch is performed by a short-term, about 30-ps-long, blueshift of the exciton energy of (In, Ga)As quantum wells in the cavity active layer by a 10-ps strain pulse generated in the GaAs substrate by a violet femtosecond laser pulse and injected into the microcavity. The proposed all-optical control of light polarization using acoustic modulation of a polariton resonance opens the way for fast and easily tunable optical polarization switches.

DOI: 10.1103/PhysRevApplied.18.044045

I. INTRODUCTION

Built-in switching devices form the basis of ultrafast optical signal processing [1,2]. The fastest intensity switching speed is achieved in all-optical switches, allowing the implementation of femtosecond all-optical devices for ultrafast communication and signal processing [1,3–6]. Recently, light-polarization switches are gaining more and more interest in connection with their application in spin-based devices [7]. The shortest processes are provided by all-optical polarization switching schemes with switching rates in the picosecond range [8–12]. The use of microcavity (MC) exciton polaritons for polarization switching provides a significant step forward due to their low-threshold polarization-dependent nonlinear radiation [13,14], fast operation, and integrability [12,15].

Exciton polaritons in semiconductor MCs are composite bosons formed due to strong exciton-photon coupling in the active layer [16–19]. They behave like a weakly nonideal Bose gas with repulsive pair interaction [17,19–22]. Due to the photon component macroscopically coherent collective states of cavity polaritons can be implemented by resonant optical driving and directly controlled by optical means. The exchange interaction between polaritons inherited from the exciton component promotes in the excited coherent polariton states a variety of collective effects such as multiple parametric scattering [23–26], solitons [27,28], spin symmetry breaking [29], pattern formation [30,31], and even turbulence [32,33]. Many of these effects originate from optical multistability induced by the blueshift of polariton resonance with increasing density due to positive feedback between the amplitude and the effective resonant frequency of the excited lower polariton (LP) mode [14,24,29,30,34–41]. The interaction of polaritons in the LP branch is highly spin dependent [42,43]. Therefore sharp transitions at critical points can occur between stationary LP states with different densities and spins resulting in the corresponding sharp switching of LP emission intensity and polarization due to their dual-exciton-photon nature.

In the present paper, we experimentally demonstrate an acoustically induced subnanosecond switching of cavity spinor LP fluid between polarized states with different degrees of circular polarization (DCP), ρ_c. The underlying mechanism is based on the effect of controlled switching between stable branches with different spin in a multistable system of resonantly excited LPs by a short-term, about 90-ps-long, blueshift of their resonance energy E_{LP}, induced by acoustic subterahertz modulation of exciton energy E_X in the quantum wells inside the active layer of the cavity. The acoustic modulation of E_X is achieved by

*alexey.shcherbakov@tu-dortmund.de
†kulakovs@issp.ac.ru

injecting into the MC a picosecond strain pulse generated by an optical pulse with a duration of 200 fs and a central photon energy $\hbar\omega = 3.1$ eV [44–46].

II. EXPERIMENTAL IDEA AND REALIZATION

A. Switching principle

The operation principle of an acoustic polariton polarization switch is as follows. The coherent LP system is prepared by resonant pumping with an external cw laser with a low DCP on the lower stability branch in a multistable state with up to four stability branches of different polarizations. The multistable state is realized when the photon energy $\hbar\omega_p$ of the pump laser is larger than E_{LP} by several $\mathrm{Im}E_{\mathrm{LP}} = \hbar\gamma$ and its power P_p is less than the critical P_{cr} for the transition of the LP system to the higher branches of stability, but more than $P^{\star}_{\mathrm{cr}}$ for the reverse transition back from them [14,36,47]. The value of P_{cr} depends on the detuning of the pump and LP modes, $\delta = \hbar\omega_p - E_{\mathrm{LP}}$, it decreases with decreasing δ. This opens up the possibility of controlling the switching of the LP state between the stability branches using a compressive strain pulse that brings the LP resonance closer to $\hbar\omega_p$ due to the blue shift of E_X. As a result, this pulse causes (i) a weak short-term reversible increase in the transmission signal when the blueshift is insufficient to decrease P_{cr} below P_p and (ii) its irreversible increase due to nonlinear transition to high-density macroscopically coherent (condensate) state on the higher branch of stability, when P_p exceeds P_{cr}.

Recently the controlled irreversible subnanosecond switching of the emission intensity of the circularly polarized LP system by more than an order of magnitude was experimentally demonstrated in GaAs-based MCs [40]. Now we show that the weak interaction between LP components with opposite spins [42,43] does not exclude the possibility to use the same technique for independent subnanosecond switching of the circularly polarized components in the LP fluid resonantly excited by elliptically polarized light.

B. Microcavity structure and experimental scheme

The acoustic switching of LP spin state is investigated in a 2λ-GaAs/AlAs MC grown by molecular-beam epitaxy on a 0.35-mm-thick GaAs substrate. It contains four sets of three 10-nm-thick $In_{0.05}Ga_{0.95}As$ quantum wells (QWs) in the active layer of 588-nm width, surrounded by distributed Bragg reflectors (DBRs) with 25 (top) and 29 (bottom) GaAs (58.8 nm)/AlAs (69.5 nm) pair stacks. The Rabi splitting $R = 7.5$ meV, the LP decay $\gamma \approx 15$ μeV.

The polariton system in the MC is photogenerated by a cw Ti:sapphire laser with photon energy $\hbar\omega_p = E_{\mathrm{LP}}(k = 0) + 100$ μeV from the substrate side by an elliptically polarized beam with degree of circular polarization $\rho_{c,p} =$ 0.2 at normal incidence. An acousto-optical modulator is used to form quasi-cw pump pulses with a duration of 35 ns and a repetition rate of 100 kHz. The laser pulses are focused to a spot of 0.15-mm diameter with an average power density $P_{\mathrm{el}} = 150$ kW/cm^2. The LP emission is detected by a streak camera in the transmission geometry to avoid any contribution from the scattered laser beam. The measurements are performed in an optical cryostat at a temperature of $T = 4.5$ K.

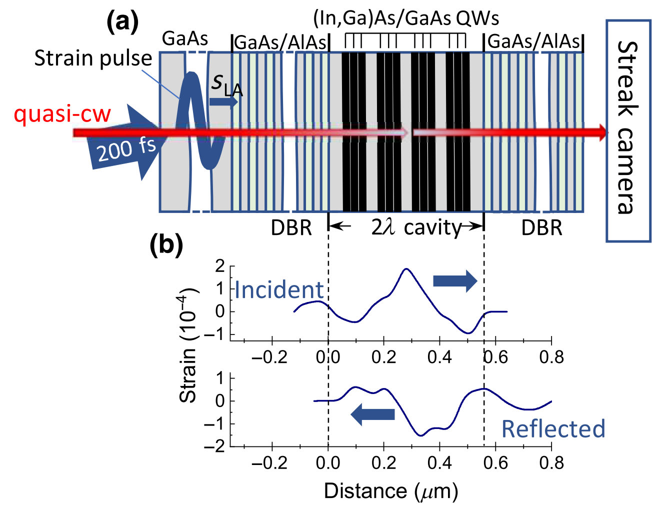

FIG. 1. (a) Schematic of microcavity structure and experiment. (b) Spatial profiles of substrate-side incident (upper panel) and reflected from top DBR-air boundary (lower panel) strain pulses at $t = 73.2$ and 74.7 ns after excitation of the GaAs substrate by a femtosecond violet pulse.

The sub-THz acoustic modulation of the LP resonance is obtained by injecting picosecond strain pulses into the MC. The pulses are generated at the substrate backside with a repetition rate of 100 kHz by 200-fs laser pulses from an amplified and frequency doubled Ti:sapphire laser at $\hbar\omega = 3.1$ eV ($\lambda = 400$ nm) as shown in Fig. 1(a). The laser pulses are focused into a spot with a diameter of 0.2 mm. Each optical pulse with excitation density W of $0.5 - 0.8$ mJ/cm^2 generates an electron-hole plasma in the near-surface GaAs layer (10 nm) and induces stress due to the combination of deformation potential and thermoelastic mechanisms. The local stress gives rise to a bipolar picosecond strain pulse that propagates away from the free surface at the speed of longitudinal sound [48–50]. Owing to the supersonic plasma diffusion during the first several picoseconds after the optical excitation, the shape of the strain pulse is strongly asymmetric [49,50]. The amplitude of its leading (compressive) peak is markedly smaller than that of the subsequent (tensile) peak [see the upper panel in Fig. 1(b)].

The strain pulse propagates in the bulk of GaAs with the velocity of longitudinal sound of $v = 4.8 \times 10^3$ m/s [51], reaches the MC active layer in 73.2 ns, propagates through it shaking subsequently four sets of three QWs and the top DBR, is reflected from the open sample surface with a π-phase shift, and returns back to the active layer with QWs in 1.5 ns and shakes the QWs again. While propagating through the substrate and DBRs, the spatiotemporal shape of the strain pulse changes due to phonon dispersion and nonlinear effects [49,50], as well as multiple reflections inside the DBR [52]. The calculated spatial distributions of the incident and reflected strain pulses inside the active layer of MC are shown in Fig. 1(b) at $t = 73.2$ and 74.7 ns, respectively, after the moment when the femtosecond laser pulse hits the substrate backside [53]. The strain pulse by means of the deformation potential modulates the QW exciton energy E_X and hence E_{LP}. To detect its effect on the LP emission, we synchronize the readout of the streak camera, as well as the femtosecond and the quasi-cw pulses with variable and controllable delays between them. The LP emission signal is measured in the transmission geometry with time resolution of 2 ns in two opposite circular polarizations.

Switching of the bistable circularly polarized LP system with the use of the sub-THz acoustic modulation of the LP resonance from the lower to the upper stable state was reported in Refs. [40,54]. There, it was shown that the blue energy shift of LP resonance induced by 30-ps-long strain pulse in the MC, pumped by a laser with $\hbar\omega_p > E_{\mathrm{LP}}$, can trigger an irreversible switch from the lower to the upper stable state, which is accompanied by an instant increase of the emission intensity by more than an order of magnitude.

The idea of acoustic switching of the spin state of a multistable optically driven spinor LP system is based on two facts. First, acoustic switching was recently implemented in a bistable circularly polarized LP system pumped resonantly by circularly polarized light [40]. Second, the much weaker interaction of LPs with opposite spins compared to the interaction of LPs with identical spins [42,43,55] opens the way for almost independent controlled switching of the two spin components.

III. EXPERIMENTAL RESULTS

The experimental realization of acoustic switching is illustrated in Fig. 2. It shows a set of time traces of the circularly polarized components of the LP emission intensities under elliptically polarized resonant excitation at $\hbar\omega_p = E_{\mathrm{LP}} + 100\ \mu$eV with and without additional excitation by a violet femtosecond pulse, recorded across a wide time interval of 65 ns with a time resolution of 2 ns. The resonant pump pulse is delayed relative to the fs pulse by $t_{\mathrm{cw}} = 62$ ns and has a plateau of almost constant intensity between 75 and 105 ns.

Time dependences of the σ components of LP radiation $I_{\mathrm{LP}}^{+,-}(t)$, measured in the absence of a strain pulse at $P_{\mathrm{el}} = 150$ kW/cm^2 and with $\rho_{c,p} = (P_{\mathrm{el}}^{+} - P_{\mathrm{el}}^{-})/(P_{\mathrm{el}}^{+} + P_{\mathrm{el}}^{-}) = 0.2$ are shown in Fig. 2(d). These intensities are

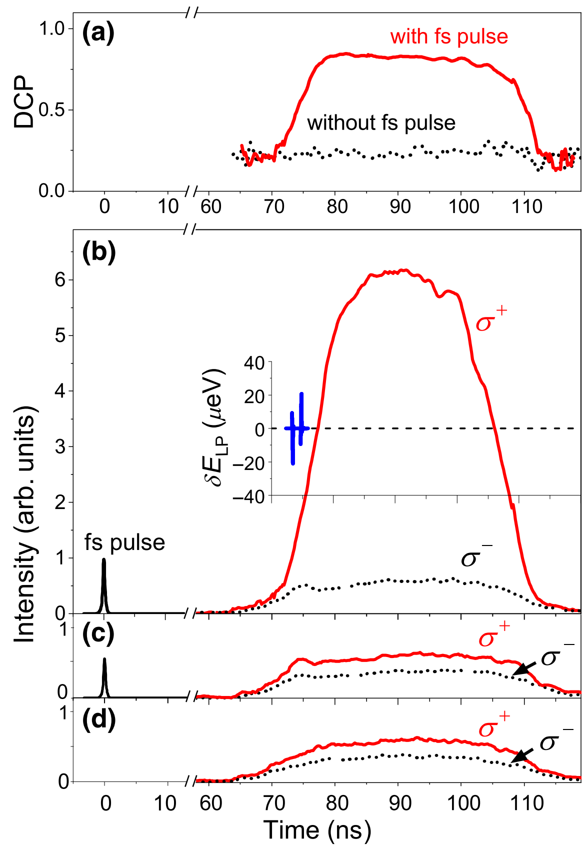

FIG. 2. (a) Time profiles of DCP in the absence (black dotted curve) and upon excitation by a femtosecond pulse with $W = 0.8$ mJ/cm^2 (red solid curve). (b)–(d) Intensities $I_{\mathrm{LP}}^{+}(t)$ (red solid curves) and $I_{\mathrm{LP}}^{-}(t)$ (black dotted curves) measured at $P_{\mathrm{el}} = 150$ kW/cm^2 for several densities of excitation by the fs pulse, W: $W = 0$ (d), 0.5 (c), and 0.8 mJ/cm^2 (b). The time resolution in these measurements is 2 ns. The inset in (b) shows the time evolution of the LP energy shift, δE_{LP}, induced by the action of the incident and reflected strain pulses at $W = 0.8$ mJ/cm^2.

about an order of magnitude lower than those recorded at $P_{\mathrm{el}} = 300$ kW/cm^2, which indicates that they correspond to the emission of LPs on the lower branch of stability. Dependences $I_{\mathrm{LP}}^{+,-}(t)$ reproduce the shape of the pump pulse, $\rho_c = (I_{\mathrm{LP}}^{+} - I_{\mathrm{LP}}^{-})/(I_{\mathrm{LP}}^{+} + I_{\mathrm{LP}}^{-}) = 0.22 \pm 0.02$ [Fig. 2(a), black dotted curve] is close to $\rho_{c,p} = 0.2$.

The situation changes when the strain pulse generated at the substrate backside by the violet 200-fs pulse is injected into the MC. The effect on the LP radiation by the strain pulse generated by the pulses with $W = 0.5$ and 0.8 mJ/cm^2 is shown in Figs. 2(c) and 2(b), respectively. The pulse with $W = 0.5$ mJ/cm^2 causes a weak short-term perturbation of both I_{LP}^{+} and I_{LP}^{-} during $t = 73 - 75$ ns, which corresponds to the transit time of the strain pulse through the QW region in the active layer of the MC. The perturbation stops when the strain pulse leaves the QW region. An increase in W up to 0.8 mJ/cm^2 leads to an irreversible 12-fold increase in the intensity of the dominant σ^+ component in I_{LP}, which persists until the end of optical pumping. The perturbation of the intensity of the weaker σ^- component remains weak and reversible. A strong irreversible increase in only one dominant component leads to an increase in the DCP of LP emission: in Fig. 2(a), it can be seen that for $t > 75$ ns, the DCP increases from 22% up to 82%.

Thus, we demonstrate that acoustic pulses can be used to rapidly switch the spin state of a cavity LP system driven by elliptically polarized light. The physics of the triggered switching of LP polarization and the range of the initial and final values of ρ_c available for the switching by the picosecond strain pulse injected into the MC from the GaAs substrate can be easily understood from consideration of the temporal evolution of strain-induced modulation of E_{LP} and S-shaped dependencies of the LP resonance on the optical excitation density P at $\hbar\omega_p > E_{\mathrm{LP}}(k=0)$.

IV. NUMERICAL MODELING

A. S-shaped dependence and its critical points

The interaction of LPs with opposite spins in GaAs MCs is about 20 times smaller than that of LPs with the same spin [42,43,55]. Therefore, one can use the S-shaped dependence of LP resonance energy on the density of optical excitation by circularly polarized light P_σ as a first approximation for the dependencies of blueshifts of the σ^+ and σ^- components in the case of elliptically polarized light with the replacement of P_σ by $P_{\mathrm{el}}(1 \pm \rho_c)/2$, respectively.

The calculated S-shaped dependence of the LP resonance on the effective pump intensity F_σ is shown in Fig. 3 by the thick solid line S0. The effective pump intensity, $F_\sigma = \alpha^2 |f|^2$, is determined by the LP oscillator strength α and the incident electric field f (i.e., $|f_\sigma|^2 \propto F_\sigma$). The dependence is calculated in the frame of a one-mode approximation when the response of the driven LP mode at fixed circularly polarized pumping density is described by the equation [35,47]

$$|\psi_\sigma|^2 = F_\sigma/[(D - V_1|\psi_\sigma|^2)^2 + \gamma^2], \tag{1}$$

where V_1 is the LP-LP interaction constant for LPs with the same spin, so that $V_1|\psi_\sigma|^2$ yields the LP resonance blueshift. The emission intensity $I_{\mathrm{LP}} \propto |\psi_\sigma|^2$. For the calculations we use $\gamma = 15$ μeV at the detuning $D = \hbar\omega_p - E_{\mathrm{LP}}(k=0) = 100$ μeV, which correspond to the investigated MC. It is seen in Fig. 2(b) that the upward transition in the LP system at $P_{el,0} = 150$ kW/cm^2 is followed by the 12-fold increase of I^+_{LP}. The critical value of F_σ corresponding to the 12-fold increase in I^+_{LP} can be determined from the curve S0 in Fig. 3, calculated for $D = 100$ μeV (black solid line S0), it is equal to 0.022 eV^2/cm^2.

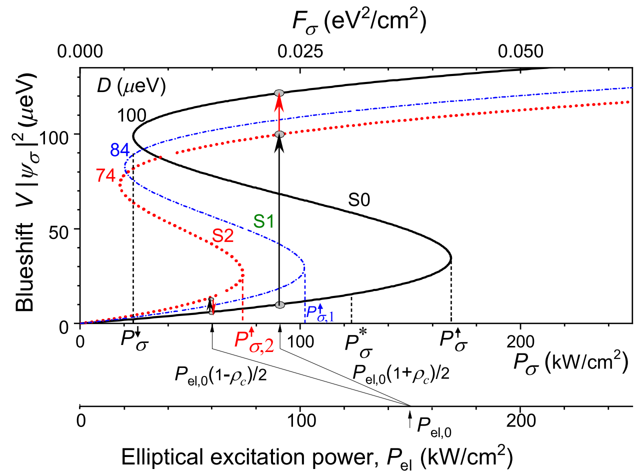

FIG. 3. S-shaped dependences of the LP resonance blueshift $\delta E_{\mathrm{LP}} = V_1|\psi_\sigma|^2$ on the excitation density of σ-polarized light, calculated for the equilibrium spectral position of the LP resonance with $D = D_0 = 100$ μeV (black solid line S0) and for the maximally shifted LP resonance by the compressive strain produced by the reflected strain pulse at $W = 0.5$ mJ/cm^2 ($D = 84$ μeV, blue dotted line S1) and $W = 0.8$ mJ/cm^2 ($D = 74$ μeV, red dotted line S2). Solid black and red arrows show the switching of a circularly polarized LP component at $W = 0.8$ mJ/cm^2 when a compression pulse passes through the quantum well region and after leaving it, respectively.

Thus we find that $P_\sigma = P_{\mathrm{el},0}(1 + \rho_{c,p})/2 = 90$ kW/cm^2 corresponds to $F_\sigma = 0.022$ eV^2/cm^2.

The critical points for the upward ($F^\uparrow_\sigma$) and downward ($F^\downarrow_\sigma$) transitions between the lower and upper stability branches are [35,47]

$$F^{\uparrow,\downarrow}_\sigma = 2[D^3 + 9D\gamma^2 \pm (D^2 - 3\gamma^2)^{3/2}]/27V_1. \tag{2}$$

In general, in planar MCs one has to include into the consideration the intermode parametric scattering of LPs that leads to a gradual growth of $|\psi|^2$ at $F > F_1 = \gamma[(D-\gamma)^2 + \gamma^2]/V_1$, and results in lowering of the threshold of upward transition at the cost of extending the duration of transition period [26,47]. In the investigated MC the value of F_1 at $D = 100$ μeV is about 0.031 eV^2/cm^2. The corresponding excitation density is indicated in Fig. 3 as P^*_σ. Figure 3 shows that P^*_σ is well above both $P_{\mathrm{el},0}(1 + \rho_{c,p})/2$ and $P_{\mathrm{el},0}(1 - \rho_{c,p})/2$. Therefore, the intermode parametric scattering of LPs can be neglected.

B. Strain-induced perturbations

The calculated temporal evolution of the strain-induced LP energy shift $\delta E_{\mathrm{LP}}(t) = E_{\mathrm{LP}}(t) - E_{\mathrm{LP}}(t=0)$ at $W = 0.5$ and 0.8 mJ/cm^2 is shown in Fig. 4. The bipolar strain pulse passing through the active layer modulates E_X in the QWs sequentially, since the extent of the compressed and stretched regions it creates (200–250 nm) is small

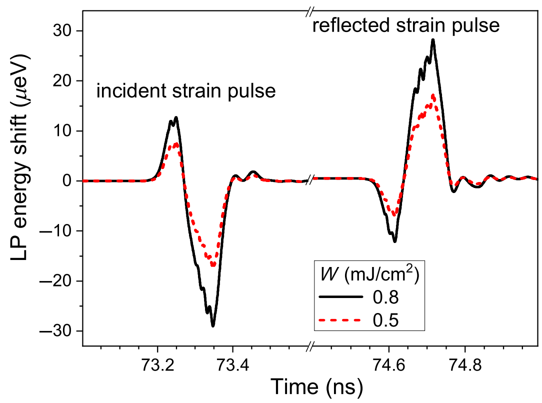

FIG. 4. Calculated temporal evolution of strain-induced modulation of the LP energy shift δE_{LP} at $W = 0.5$ and $0.8\ \mathrm{mJ/cm^2}$.

compared to the width of the active layer $2\lambda = 588$ nm [Fig. 1(b)]. Thus, the pulse simultaneously produces a blueshift of E_X in some QWs, a redshift in others, and leaves some QWs unchanged. The effect of the E_X perturbations in the QWs on the variation of the LP resonance is averaged over all QWs in the spacer. As a result, the duration of the perturbation of $E_{\mathrm{LP}}(t)$ increases. The dependences of $\delta E_{\mathrm{LP}}(t)$ shown in Fig. 4 are calculated taking into account the temporal variation of E_X in all QWs and the deformation potential $\Xi = -1$ eV [50]. It is seen in Fig. 4 that the successive passage of the strain pulse through the four groups of QWs located with a period of $\lambda/2$ leads to relatively weak, approximately 10% magnitude, oscillations in $\delta E_{\mathrm{LP}}(t)$ with a period of $T_1 = \lambda/2v \sim 20$ ps. These oscillations are too small to cause any sequential switching of the LP system, and, moreover, their effect on the polariton mode is strongly averaged, since $T_1 \sim 20$ ps is an order of magnitude smaller than the decay time, $1/\gamma = 250$ ps. Besides, it is worthwhile to mention that a high-Q GaAs/AlAs MC for near-IR light is also a high-Q cavity for longitudinal acoustic phonons with the same wavelength [56], for which strong coupling with a polariton condensate has been demonstrated [57,58]. However, excitation of this phonon mode by the strain pulse injected into the MC has low efficiency [59] and, thus, it does not affect the state of polaritons.

Figure 4 shows that the perturbation of E_{LP} induced by the incident pulse begins with its short, about 30 ps lasting, increase at $t = 73.2$ ps and ends with its short-term, approximately 90-ps-long, decrease when, respectively, the compressive and then the tensile peaks of the strain pulse disturb E_X in the quantum wells. In 1.5 ns, the strain pulse reflected from the open surface of the sample with a π-phase shift returns back to the active layer with QWs. This pulse begins with a short tensile peak that causes a 30-ps decrease in E_{LP} and ends with a compressive peak that leads to its short-term, about 90-ps-long, blueshift.

The switching of the LP system from the lower to upper stability branch is induced by the blueshift of E_{LP}, induced by the compressive peak of the strain pulse. It is seen in Fig. 4 that the blueshift of E_{LP} induced by the reflected pulse is the last significant perturbation of the MC, and it is about twice as large as that induced by the incident strain pulse. The blueshifts of $\delta E_{\mathrm{LP}} \sim 16$ and 26 μeV, which are induced by the reflected pulse at $W = 0.5$ and $0.8\ \mathrm{mJ/cm^2}$, lower D from 100 μeV to 84 and 74 μeV, respectively. The S-shaped dependencies of the LP resonance on P_σ at $D = 84$ and 74 μeV are shown in Fig. 3 by the curves S1 and S2, respectively. It is seen that both $P_{\mathrm{el},0}(1 \pm \rho_c)/2$ are less than the threshold value $P^{\uparrow}_{\sigma,1} = 102\ \mathrm{kW/\ cm^2}$ at $D = 84\ \mu$eV. As a consequence, the strain pulse at $W = 0.5\ \mathrm{mJ/cm^2}$ leads to a weak short-term perturbation of both σ^+ and σ^- components of LP emission as observed in experiment [Fig. 2(c)].

Figure 4 shows that the compressive peak in the incident strain pulse at $W = 0.8\ \mathrm{mJ/cm^2}$ shifts E_{LP} by less than that in the reflected pulse at $W = 0.5\ \mathrm{mJ/cm^2}$. Hence, it can cause only a weak short-term perturbation of LP emission. Thus, the observed switching between the lower and upper stability branches at $W = 0.8\ \mathrm{mJ/cm^2}$ is caused by the compressive peak in the reflected pulse. This peak shifts E_{LP} by 26 meV, and leads to lowering of the critical density $P^{\uparrow}_{\sigma}$ down to $P^{\uparrow}_{\sigma,2} = 73\ \mathrm{kW/cm^2}$ that falls in between $P_{\sigma^-,0} = P_{\mathrm{el},0}(1 - \rho_{c,p})/2$ and $P_{\sigma^+,0} = P_{\mathrm{el},0}(1 + \rho_{c,p})/2$ (60 and 90 $\mathrm{kW/cm^2}$, respectively).

Since $P_{\sigma^-,0} < P^{\uparrow}_{\sigma}$, this compressive peak causes the transition of the minor component σ^- from the initial state on the lower branch S0 to that in S2 with a small increase in $V_1|\psi^-|^2$ to approximately equal to 13.5 μeV (thin black arrow in Fig. 3). As a result, after the end of strain pulse, this component finds itself in the basin of attraction of the lower branch of stability on the S0 curve and returns back to its original state with $V_1|\psi^-|^2 \approx 6.2\ \mu$eV. The influence of the compression peak on the dominant σ^+ component is directly opposite. Since $P_{\sigma^+,0} > P^{\uparrow}_{\sigma}$, this peak causes the transition of the σ^+ component from the initial state with $V_1|\psi^+|^2 \approx 10\ \mu$eV on S0 into a high density state ($V_1|\psi^+|^2 \approx 100\ \mu$eV) on the upper branch S-shaped curve S2 (black solid arrow in Fig. 3). This state is located in the basin of attraction of the upper branch of stability of the S-shaped dependence S0 in the MC with unstrained quantum wells. Therefore, after the end of strain pulse, the σ^+ component passes to it, followed by an increase in $V_1|\psi^+|^2$ up to 120 μeV (red solid arrow in Fig. 3). As a result, after passing through the compression peak, the DCP of LP emission increases from 0.22 to 0.82, as shown in Fig. 2(a). Thus, one of the two spin components is amplified nearly independently of the other, which is the foundation of the very possibility of polarization conversion.

C. Effect of spin relaxation

Finally, it should be noted that the comparison of Figs. 2(b) and 2(d) shows that the intensity of the minor

LP component $I^-_{\rm LP}(t)$ after switching $I^+_{\rm LP}(t)$ is somewhat, approximately $15-20\%$, greater than its intensity measured in the absence of the $I^+_{\rm LP}(t)$ jump at $W=0$ and $0.5\ {\rm mJ/cm^2}$. Note that even such an insignificant increase in the minor component contradicts the conventional assumption of an attractive character of the interaction between σ^+ and σ^- LPs. Indeed, attractive interaction should involve a redshift of resonance energy and, thus, a decrease in amplitude of the minor component in response to the jump in the major one. And vice versa, the observed growth in $I^-_{\rm LP}$ is indicative of a certain kind of repulsive ("blueshifting") opposite-spin interaction. This anomalous blueshift was in fact observed earlier in the framework of all-optical multistability experiments (with no strain pulses) and was attributed to the weak scattering of optically driven LPs into a long-lived incoherent exciton reservoir, in which exciton spin relaxation occurs much faster than the exciton decay in the reservoir (approximately 300 ps) [38,60,61].

The depolarized reservoir provides the same blueshift for both coherent spin states, in addition to their redshift due to the attractive interaction between them. The dominant channel for polariton transitions from coherently controlled modes to the reservoir is the scattering of LPs with opposite σ polarizations [38,61]. Therefore, the temporal behavior of the exciton density in the reservoir N_X can be described by the equation

$$dN_X/dt \approx -N_X/\tau_X + 4V_r n^+_{\rm LP} n^-_{\rm LP}, \tag{3}$$

that gives for $t > 3\tau_X$ the stationary value $N_X = (4V_r n^+_{\rm LP} n^-_{\rm LP})/\tau_X$, where τ_X is the exciton lifetime and V_r is the constant of the effective pair interaction of LPs with opposite polarizations with densities $n^+_{\rm LP}$ and $n^+_{\rm LP}$, respectively. Thus, the filling of the reservoir will change the redshift to a blueshift at $(2V_r n^-_{\rm LP})\tau_X > |V_2|/(V_1+V_2) \sim 1/20$ in the GaAs MC. In all-optical multistability experiments with no strain pulses, the switching of the LP polarization is usually accompanied by a similar switching of the minor component after several hundred ps and the return of the LP polarization to a state close to linear due to the high density of the minor LP component [36,38,55,62–64]. The use of strain pulses makes it possible to significantly reduce $n^-_{\rm LP}$ by reducing the critical density $P^\uparrow_\sigma$ and thereby reduce the blueshift of the minor LP component to a minimum as well as make the polarization switching irreversible.

Thus, the experimentally realized switching of DCP from 0.22 up to 0.82 by picosecond acoustic pulses is well explained in the approximation of weakly interacting LP subsystems with opposite spins. Within this approximation, polarization switching occurs under the condition that $P_{\rm el,0}(1-\rho_{c,p})/2 < P^\uparrow_\sigma(D-\delta E_{\rm LP}) < P_{\rm el,0}(1+\rho_{c,p})/2$. Therefore, the minimum value of ρ_c in the initial state $\rho_{c,\rm in}$ is mainly determined by fluctuations in the intensity of pumping cw and fs lasers. A $\rho_{c,\rm in}$ as small as 0.05 can be experimentally reached if these fluctuations are within 2%. As to the maximal degree of circular polarization in the final state $\rho_{c,\rm max}$, it is determined by the magnitude of the jump in the $|\psi|^2$ of dominant LP component upon switching. The ratio of LP densities on the upper and lower stability branches, $n_{\rm LP,up}/n_{\rm LP,low}$ increases with lowering $P_{\rm el}(1+\rho_c)/2$ down to $P^\downarrow_\sigma(D)$. A ρ_c as high as 0.9 can be realized in high-Q MCs at $\gamma/D < 0.15$, even at $\rho_{c,\rm in} \sim 0.05$.

V. CONCLUSIONS

In conclusion, we demonstrate all-optical ultrafast polarization switches between steady states in a GaAs-based microcavity under resonant cw excitation, using optically generated strain pulses with a duration of 30 ps, which cause a short-term reversible perturbation of the exciton energy. The switching is possible when two conditions are satisfied simultaneously, namely, (i) the pump frequency detuning is several times greater than ${\rm Im}E_{\rm LP} = \hbar\gamma$ (i.e., the polariton system is resonantly excited in a multistable regime), and (ii) the duration of the acoustic pulses is comparable to the polariton lifetime $1/\gamma$. Therefore, it may be suggested that acoustic control of polariton polarization can be realized even at room temperature in MCs based on wide-gap materials such as GaN, ZnO, 2D dichalcogenides, and perovskites, in which the two above conditions can be obeyed employing state-of-the-art technology.

The proposed acoustic control of the polariton polarization in the cavity has clear advantages over the optical triggering of the transition in the LP system using resonant laser pulses, since its implementation does not require phase synchronization of two beams. In the investigated MCs with a spin degenerate LP state this makes it possible to realize controlled switching of polarization in a wide DCP range from 0.05–0.80 in the initial state to 0.7–0.9 in the final state. A strong expansion of this range is expected in the case of strained MCs with lifted degeneracy of the LP state. In particular, a reversal of the condensate spin in both directions in response to identical deformation pulses under constant excitation of strained MCs was predicted in Ref. [65]. Thus, all-optical control of light polarization using acoustic modulation of LP resonance opens the way for fast and highly tunable optical polarization switches.

ACKNOWLEDGMENTS

We are grateful to P. Savvidis for the high-Q MC and to N.A. Gippius and A.V. Akimov for valuable discussions. The work is supported by the Deutsche Forschungsgemeinschaft (Grant No. TRR 142 project A06), the Volkswagen Foundation (Grant No. 97758), and the International Collaborative Research Center TRR 160 (Projects A1 and B7). S.S.G. and V.D.K. also acknowledge the support by the Russian Science Foundation (Grant RSF 21-12-00368)

[1] O. Wada, Femtosecond all-optical devices for ultrafast communication and signal processing, New J. Phys. **6**, 183 (2004).

[2] J. L. O'Brien, A. Furusawa, and J. Vuckovic, Photonic quantum technologies, Nat. Photonics **3**, 687 (2009).

[3] R. Takahashi, Y. Kawamura, and H. Iwamura, Ultrafast 1.55 mm all-optical switching using low-temperature-grown multiple quantum wells, Appl. Phys. Lett. **68**, 153 (1996).

[4] J. Liu, M. Beals, A. Pomerene, S. Bernardis, R. Sun, J. Cheng, L. C. Kimerling, and J. Michel, Waveguide-integrated, ultralow-energy GeSi electro-absorption modulators, Nat. Photonics **2**, 433 (2008).

[5] M. Steger, C. Gautham, B. Nelsen, D. Snoke, L. Pfeiffer, and K. West, Single-wavelength, all-optical switching based on exciton-polaritons, Appl. Phys. Lett. **101**, 131104 (2012).

[6] D. Sanvitto and S. Kena-Cohen, The road towards polaritonic devices, Nat. Mater. **15**, 1061 (2016).

[7] I. Zutic, J. Fabian, and S. Das Sarma, Spintronics: Fundamentals and applications, Rev. Mod. Phys. **76**, 323 (2004).

[8] Y. Nishikawa, A. Tackeuchi, M. Yamaguchi, S. Muto, and O. Wada, Ultrafast all-optical spin polarization switch using quantum-well etalon, IEEE J. Sel. Top Quantum Electron. **2**, 661 (1996).

[9] R. Takahashi, H. Itoh, and H. Iwamura, Ultrafast high-contrast all-optical switching using spin polarization in low-temperature-grown multiple quantum wells, Appl. Phys. Lett. **77**, 2958 (2000).

[10] M. Yildirim, J. P. Prineas, E. J. Gansen, and A. L. Smirl, A near-room-temperature all-optical polarization switch based on the excitation of spin-polarized "virtual" carriers in quantum wells, J. Appl. Phys. **98**, 063506 (2005).

[11] W. J. Johnston, J. P. Prineas, and A. L. Smirl, Ultrafast all-optical polarization switching in Bragg-spaced quantum wells at 80 K, J. Appl. Phys. **101**, 046101 (2007).

[12] A. Amo, T. C. H. Liew, C. Adrados, R. Houdre, E. Giacobino, A. V. Kavokin, and A. Bramati, Exciton-polariton spin switches, Nat. Photon. **4**, 361 (2010).

[13] M. D.Martin, G. Aichmayr, L. Vina, and R. Andre, Polarization Control of the Nonlinear Emission of Semiconductor Microcavities, Phys. Rev. Lett. **89**, 077402 (2002).

[14] N. A. Gippius, I. A. Shelykh, D. D. Solnyshkov, S. S. Gavrilov, Y. G. Rubo, A. V. Kavokin, S. G. Tikhodeev, and G. Malpuech, Polarization Multistability of Cavity Polaritons, Phys. Rev. Lett. **98**, 236401 (2007).

[15] D. Ballarini, M. De Giorgi, E. Cancellieri, R. Houdre, E. Giacobino, R. Cingolani, A. Bramati, G. Gigli, and D. Sanvitto, All-optical polariton transistor, Nat. Commun. **4**, 1778 (2013).

[16] C. Weisbuch, M. Nishioka, A. Ishikawa, and Y. Arakawa, Observation of the Coupled Exciton-Photon Mode Splitting in Semiconductor Quantum Microcavity, Phys. Rev. Lett. **69**, 3314 (1992).

[17] D. Sanvitto and V. Timofeev, *Exciton Polaritons in Microcavities* (Springer-Verlag, Berlin, 2012).

[18] Benoit Deveaud, *The Physics of Semiconductor Microcavities* (WILEY-VCH, Weinheim, 2007).

[19] A. V. Kavokin, J. J. Baumberg, G. Malpuech, and P. Laussy, *Microcavities* (Oxford University Press, New York, 2017), 2nd ed.

[20] K. Lagoudakis, *The Physics of Exciton-Polariton Condensates* (EPFL Press, Lausanne, 2013).

[21] A. Bramati and M. Modugno, *Physics of Quantum Fluids* (Springer-Verlag, Berlin, 2013).

[22] H. Deng, H. Haug, and Y. Yamamoto, Exciton-polariton Bose-Einstein condensation, Rev. Mod. Phys. **82**, 1489 (2010).

[23] R. M. Stevenson, V. N. Astratov, M. S. Skolnick, D. M. Whittaker, M. Emam-Ismail, A. I. Tartakovskii, P. G. Savvidis, J. J. Baumberg, and J. S. Roberts, Continuous Wave Observation of Massive Polariton Redistribution by Stimulated Scattering in Semiconductor Microcavities, Phys. Rev. Lett. **85**, 3680 (2000).

[24] N. A. Gippius, S. G. Tikhodeev, V. D. Kulakovskii, D. N. Krizhanovskii, and A. I. Tartakovskii, Nonlinear dynamics of polariton scattering in semiconductor microcavity: Bistability vs. stimulated scattering, Europhys. Lett. **67**, 997 (2004).

[25] A. A. Demenev, A. A. Shchekin, A. V. Larionov, S. S. Gavrilov, V. D. Kulakovskii, N. A. Gippius, and S. G. Tikhodeev, Kinetics of Stimulated Polariton Scattering in Planar Microcavities: Evidence for a Dynamically Self-Organized Optical Parametric Oscillator, Phys. Rev. Lett. **101**, 136401 (2008).

[26] S. S. Gavrilov, A. S. Brichkin, Y. V. Grishina, C. Schneider, S. Höfling, and V. D. Kulakovskii, Blowup dynamics of coherently driven polariton condensates: Experiment, Phys. Rev. B **92**, 205312 (2015).

[27] O. A. Egorov, D. V. Skryabin, A. V. Yulin, and F. Lederer, Bright Cavity Polariton Solitons, Phys. Rev. Lett. **102**, 153904 (2009).

[28] M. Sich, D. V. Skryabin, and D. N. Krizhanovskii, Soliton physics with semiconductor exciton-polaritons in confined systems, C. R. Phys. **17**, 908 (2016).

[29] S. S. Gavrilov, A. V. Sekretenko, S. I. Novikov, C. Schneider, S. Höfling, M. Kamp, A. Forchel, and V. D. Kulakovskii, Polariton multistability and fast linear-to-circular polarization conversion in planar microcavities with lowered symmetry, Appl. Phys. Lett. **102**, 011104 (2013).

[30] I. A. Shelykh, T. C. H. Liew, and A. V. Kavokin, Spin Rings in Semiconductor Microcavities, Phys. Rev. Lett. **100**, 116401 (2008).

[31] C. E. Whittaker, B. Dzurnak, O. A. Egorov, G. Buonaiuto, P. M. Walker, E. Cancellieri, D. M. Whittaker, E. Clarke, S. S. Gavrilov, M. S. Skolnick, and D. N. Krizhanovskii, Polariton Pattern Formation and Photon Statistics of the Associated Emission, Phys. Rev. X **7**, 031033 (2017).

[32] S. S. Gavrilov, Towards spin turbulence of light: Spontaneous disorder and chaos in cavity-polariton systems, Phys. Rev. B **94**, 195310 (2016).

[33] S. S. Gavrilov, Polariton Chimeras: Bose-Einstein Condensates with Intrinsic Chaoticity and Spontaneous

Long-Range Ordering, Phys. Rev. Lett. **120**, 033901 (2018).

[34] V. F. Elesin and Y. V. Kopaev, Bose condensation of excitons in a strong magnetic field, Sov. Phys. JETP **36**, 767 (1973).

[35] A. Baas, J. P. Karr, H. Eleuch, and E. Giacobino, Optical bistability in semiconductor microcavities, Phys. Rev. A **69**, 023809 (2004).

[36] S. S. Gavrilov, N. A. Gippius, S. G. Tikhodeev, and V. D. Kulakovskii, Multistability of the optical response in a system of quasi-two-dimensional exciton polaritons, JETP **110**, 825 (2010).

[37] T. K. Paraiso, M. Wouters, Y. Leger, F. Morier-Genoud, and B. Deveaud-Pledran, Multistability of a coherent spin ensemble in a semiconductor microcavity, Nat. Mater. **9**, 655 (2010).

[38] D. Sarkar, S. S. Gavrilov, M. Sich, J. H. Quilter, R. A. Bradley, N. A. Gippius, K. Guda, V. D. Kulakovskii, M. S. Skolnick, and D. N. Krizhanovskii, Polarization Bistability and Resultant Spin Rings in Semiconductor Microcavities, Phys. Rev. Lett. **105**, 216402 (2010).

[39] C. Adrados, A. Amo, T. C. H. Liew, R. Hivet, R. Houdre, E. Giacobino, A. V. Kavokin, and A. Bramati, Spin Rings in Bistable Planar Semiconductor Microcavities, Phys. Rev. Lett. **105**, 216403 (2010).

[40] A. A. Demenev, D. D. Yaremkevich, A. V. Scherbakov, S. M. Kukhtaruk, S. S. Gavrilov, D. R. Yakovlev, V. D. Kulakovskii, and M. Bayer, Ultrafast strain-induced switching of a bistable cavity-polariton system, Phys. Rev. B. **100**, 100301(R) (2019).

[41] S. S. Gavrilov, Nonequilibrium transitions, chaos, and chimera states in exciton polariton systems, Phys.-Usp. **63**, 123 (2020).

[42] P. Renucci, T. Amand, X. Marie, P. Senellart, J. Bloch, B. Sermage, and K. V. Kavokin, Microcavity polariton spin quantum beats without a magnetic field: A manifestation of Coulomb exchange in dense and polarized polariton systems, Phys. Rev. B **72**, 075317 (2005).

[43] M. Vladimirova, S. Cronenberger, D. Scalbert, K. V. Kavokin, A. Miard, A. Lemaítre, J. Bloch, D. Solnyshkov, G. Malpuech, and A. V. Kavokin, Polariton-polariton interaction constants in microcavities, Phys. Rev. B **82**, 075301 (2010).

[44] A. V. Akimov, A. V. Scherbakov, D. R. Yakovlev, C. T. Foxon, and M. Bayer, Ultrafast Band-Gap Shift Induced by a Strain Pulse in Semiconductor Heterostructures, Phys. Rev. Lett. **97**, 037401 (2006).

[45] A. V. Scherbakov, T. Berstermann, A. V. Akimov, D. R. Yakovlev, G. Beaudoin, D. Bajoni, I. Sagnes, J. Bloch, and M. Bayer, Ultrafast control of light emission from a quantum-well semiconductor microcavity using picosecond strain pulses, Phys. Rev. B **78**, 241302(R) (2008).

[46] T. Berstermann, A. V. Scherbakov, A. V. Akimov, D. R. Yakovlev, N. A. Gippius, B. A. Glavin, I. Sagnes, J. Bloch, and M. Bayer, Terahertz polariton sidebands generated by ultrafast strain pulses in an optical semiconductor microcavity, Phys. Rev. B **80**, 075301 (2009).

[47] S. S. Gavrilov, Blowup dynamics of coherently driven polariton condensates, Phys. Rev. B **90**, 205303 (2014).

[48] C. Thomsen, H. T. Grahn, H. J. Maris, and J. Tauc, Surface generation and detection of phonons by picosecond light pulse, Phys. Rev. B **34**, 4129 (1986).

[49] O. B. Wright, B. Perrin, O. Matsuda, and V. E. Gusev, Ultrafast carrier diffusion in gallium arsenide probed with picosecond acoustic pulses, Phys. Rev. B **64**, 081202(R) (2001).

[50] E. S. K. Young, A. V. Akimov, R. P. Campion, A. J. Kent, and V. V. Gusev, Picosecond strain pulses generated by a supersonically expanding electron-hole plasma in GaAs, Phys. Rev. B **86**, 155207 (2012).

[51] J. S. Blakemore, Semiconducting and other major properties of gallium arsenide, J. Appl. Phys. **53**, R123 (1982).

[52] C. Brüggemann, A. V. Akimov, A. V. Scherbakov, M. Bombeck, C. Schneider, S. Höfling, A. Forchel, D. R. Yakovlev, and M. Bayer, Laser mode feeding by shaking quantum dots in a planar microcavity, Nat. Photon. **6**, 30 (2012).

[53] For the calculation of the strain temporal evolution inside the MC we used the COMSOL Multiphysics software (ver. 5.4). The data from Ref. [50] are used for setting the initial (at the first interface of bottom DBR) strain pulse after its propagation through the GaAs substrate.

[54] S. S. Gavrilov and N. A. Gippius, Pulsed acousto-optic switching of a bistable cavity polariton system, Phys. Rev. B **86**, 085317 (2012).

[55] A. V. Sekretenko, S. S. Gavrilov, and V. D. Kulakovskii, Polariton-polariton interactions in microcavities under a resonant 10 to 100 picosecond pulse excitation, Phys. Rev. B **88**, 195302 (2013).

[56] A. Fainstein, N. D. Lanzillotti-Kimura, B. Jusserand, and B. Perrin, Strong Optical-Mechanical Coupling in a Vertical GaAs/AlAs Microcavity for Subterahertz Phonons and Near-Infrared Light, Phys. Rev. Lett. **110**, 037403 (2013).

[57] D. L. Chafatinos, A. S. Kuznetsov, S. Anguiano, A. E. Bruchhausen, A. A. Reynoso, K. Biermann, P. V. Santos, and A. Fainstein, Polariton-driven phonon laser, Nat. Commun. **11**, 4552 (2020).

[58] A. A. Reynoso, G. Usaj, D. L. Chafatinos, F. Mangussi, A. E. Bruchhausen, A. S. Kuznetsov, K. Biermann, P. V. Santos, and A. Fainstein, Optomechanical parametric oscillation of a quantum light-fluid lattice, Phys. Rev. B **105**, 195310 (2022).

[59] A. Huynh, B. Perrin, N. D. Lanzillotti-Kimura, B. Jusserand, A. Fainstein, and A. Lemaître, Subterahertz monochromatic acoustic wave propagation using semiconductor superlattices as transducers, Phys. Rev. B **78**, 233302 (2008).

[60] A. Vinattieri, Jagdeep Shah, T. C. Damen, D. S. Kim, L. N. Pfeiffer, M. Z. Maialle, and L. J. Sham, Exciton dynamics in GaAs quantum wells under resonant excitation, Phys. Rev. B **50**, 10868 (1994).

[61] S. S. Gavrilov, A. S. Brichkin, A. A. Dorodnyi, S. G. Tikhodeev, N. A. Gippius, and V. D. Kulakovskii, Polarization instability in a polariton system in semiconductor microcavities, JETP Lett. **92**, 171 (2010).

[62] S. S. Gavrilov, A. S. Brichkin, A. A. Demenev, A. A. Dorodnyy, S. I. Novikov, V. D. Kulakovskii, S. G. Tikhodeev, and N. A. Gippius, Bistability and nonequilibrium transitions in the system of cavity polaritons under

nanosecond-long resonant excitation, Phys. Rev. B **85**, 075319 (2012).

[63] P. Stepanov, I. Amelio, J-G. Rousset, J. Bloch, A. Lemaitre, A. Amo, A. Minguzzi, I. Carusotto, and M. Richard, Dispersion relation of the collective excitations in a resonantly driven polariton fluid, Nat. Commun. **10**, 3869 (2019).

[64] M. Wouters, T. K. Paraiso, Y. Léger, R. Cerna, F. Morier-Genoud, M. T. Portella-Oberli, and B. Deveaud-Plédran, Influence of a nonradiative reservoir on polariton spin multistability, Phys. Rev. B **87**, 045303 (2013).

[65] S. S. Gavrilov, A. A. Demenev, and V. D. Kulakovskii, On the possibility of acousto-optic control of spin states of a polariton condensate, JETP Lett. **100**, 817 (2014).